Appendix E. Details of Groundwater-Flow Simulation

The MODFLOW numerical finite-difference model is an implementation of the conceptual model of the system. This appendix covers the additional technical details of the groundwater-flow simulation completed for this study, and the major topics covered are: (1) the method of representing each of the major flow features; (2) formulation of the model problem for each of the scenarios examined; (3) constraints placed on each model formulation (observations, parameterization, and regularization); (4) model scenario results; and (5) limitations of the model(s).

E.1—Model Grid Design

The model area was discretized into 500-ft sided square grid cells of variable thicknesses, resulting in 100 rows, 120 columns, and 14 layers. Temporal discretization was annual stress periods for the fully transient model, but the modified transient analysis simulates conditions during three distinct periods. Groundwater flow was simulated with MODFLOW-2000 using the Layer Property Flow (LPF) package (Harbaugh and others, 2000). Except for the overburden units, each of the fourteen model layers represents one of the groundwater-flow model units (fig. 3). The overburden was zoned laterally (figs. 3–5) to test the likelihood that glaciofluvial deposits in the OWRD management area limited flow rate during aquifer leakage through commingling wells. The resulting model has 168,000 cells of which 66,600 are active.

The final model grid is rotated 38 degrees clockwise to correspond with major structural features that are known to control flow, namely the Rocky Prairie thrust fault, the Columbia Hills anticline, and the Maupin wrench fault (fig. 22). This aligns the grid with the faults bounding the area of principal interest, which contains the OWRD administrative area and most of the study area water supply wells.

E.2—Additional Details for Model Boundary Conditions

Simulated model boundaries are shown in figs. 22 and A9–A22. Simulated boundaries are discussed in the Model Discretization and Boundaries section of the report, but additional details of simulation of faults, streams, and commingling wells are provided here.

Simulation of Faults

The simulated faults are a simplification of mapped faults and all faults are modeled as vertical, so data collected or modeled in close proximity to modeled barriers inherently contains more uncertainty. The overburden is assumed to be easily deformed, and even if faulting has occurred post-deposition, it is assumed that the faults themselves do not impede flow in the overburden, so no horizontal flow barriers are simulated in layers 1 and 2.

Simulated faults are continuous and span the entire model area, even if offset is small. In areas where faults have small vertical offset, the role of the fault in impeding flow is possibly small. To test whether faults impede flow to varying degrees based on offset or style of faulting, simulated faults were divided into sections (fig. 22). For example, fault sections 31, 32, and 33 represent a gradation from relatively small offset to much larger offset. In this case, section 33 is expected to have relatively lower hydraulic conductance across the fault than section 31.

The simulated faults can also exhibit different hydraulic conductance that varies with depth. For example, at the Rocky Prairie thrust fault, the overthrust thickness corresponds to detachment at the Selah interbed, indicating that older aquifers may still be continuous. As a result, the simulated faults were divided vertically into six groups that allowed testing of fault conductance with depth. Each group contains only one basalt aquifer because these are the preferential groundwater flow paths. The numbering scheme for fault hydraulic characteristic (MODFLOW parameter controlling fault hydraulic conductance) for each fault section is annotated using a single string beginning with “hf” followed by upper layer, lower layer, and fault section in plan view. For example, hf30422 is horizontal flow barrier section impeding flow through layers 3 and 4 along section 22. This provided 48 fault sections that allowed testing of the importance of faults in controlling groundwater flow during the calibration process. Faults are known to be highly important in this flow system (Newcomb, 1969, Lite and Grondin, 1988) and this was the largest set of independent parameters tested with this model. Initial values and regularization constraints are discussed in the parameter estimation section below.

Simulation of Streams

Streams were modeled using a combination of the stream and drain packages (Prudic, 1989; Harbaugh and others, 2000). For the incised streams in the study area, streams flow

across large expanses of impermeable CRBG lava flow interior rock, intersecting the thin aquifers relatively infrequently. This provides little opportunity for direct stream loss to the aquifer, but many opportunities for springs and seeps to contribute to streamflow. In model cells containing streams, this preferential gain of streamflow was modeled by setting the drain elevation to the stream stage, resulting in the following formulation of streamflow loss to the aquifer system ($Q_{total\_leakage}$):

$$Q_{total\_leakage} = (C_{stream} + C_{drain})(H_{stream} - H_{aquifer})$$

for

$$H_{stream} < H_{aquifer}, \quad \text{(E.1)}$$

$$Q_{total\_leakage} = C_{stream}(H_{stream} - H_{aquifer})$$

for

$$Z \le H_{aquifer} \le H_{stream}, \quad \text{(E.2)}$$

$$Q_{total\_leakage} = C_{stream}(H_{stream} - Z)$$

for

$$Z > H_{aquifer}, \quad \text{(E.3)}$$

where

Z is the elevation of the stream bottom,

$H_{aquifer}$ is the hydraulic head in the aquifer,

H_{stream} is the stream stage,

C_{stream} is the stream conductane, and

C_{drain} is the drain conductance.

During parameter estimation, the stream and drain conductance were varied as a function of geology. Each conductance can be written as (McDonald and Harbaugh, 1984):

$$C = \frac{KLW}{M}, \quad \text{(E.4)}$$

where

L is the length of the stream or drain,

W is the corresponding width,

M is the thickness across which most of the head loss will occur, and

K is the corresponding hydraulic conductivity.

For each model cell, the length of a stream depends on the path across the cell, and conductance is linearly dependent on the path length. Because this is the only part of the equation that is well known, the dependence on stream length is made explicit, but the other three terms are lumped and treated as a single adjustable parameter during estimation.

In addition to using drains in stream cells, drains were also used at erosional or depositional margins where water may freely drain from hydrogeologic units. For drains occurring in stream model cells, stream geometry also could be used in the parameterization, however the geometry of drains at layer margins is less precisely defined. Rather than treating drains differently at streams and layer margins, a constant length is assumed for all drains, and the drain conductance was varied as a single parameter during parameter estimation.

Because the stream package does not allow water to be routed from drains into the stream, it was necessary to add all drainage and net stream gain to compute $Q_{total\_leakage}$ for comparison with stream-flux calibration targets. This was accomplished by using ZONEBUDGET (Harbaugh, 1990) where each zone is defined to include all cells that can drain to a stream above the associated stream flux target.

Simulation of Commingling Wells

Initially, the multi-node well package (Halford and Hanson, 2002) was used to represent wells in the model, but resulting numerical instability resulted in frequent non-convergence and significant hydraulic budget errors, making use of this package impractical. The chief cause of instability for this model is that the multi-node well (MNW) package solves the groundwater flow equations and intra-borehole fluxes iteratively. Oscillatory behavior of the flow equation solver resulted because the model cell size is small, the hydraulic conductivity contrasts are large, and the storage terms are small. In the event of solver convergence problems, Halford and Hanson (2002) recommend modeling commingling of wells by varying the vertical conductance of cells that contain commingling wells, and modeling pumping using the standard well package (Harbaugh and others, 2000). This has the net effect of moving all commingling and pumping effects into the main MODFLOW equations, rather than requiring iterative solution.

This fix was implemented, and model stability and robustness were greatly improved, allowing investigation of the full range of commingling effects. However, two limitations were imposed on the model analysis by this choice. First, a full transient analysis became impractical, because commingling wells were installed gradually over many years, and hydraulic conductivity is not a time-varying parameter in MODFLOW. As a result, a modified transient analysis was used. Second, the MNW package allows water to be supplied by each cross-connected aquifer as a function of pumping

stress on the commingled well, whereas the standard well package requires that pumping stress be applied to each layer individually. To distribute this pumping, it was assumed that the amount of water supplied from each layer was proportional to the fraction of the total transmissivity represented by each layer. Mathematically, the fraction of pumping taken from layer *j* is:

$$Q_j = Q_{well} \frac{K_j b_j}{\sum_{n=1}^{N} K_n b_n}, \quad \text{(E.5)}$$

where

Q_{well} is the pumping rate of the well,

K is the horizontal conductivity of the layer,

b is the thickness of the layer at the well location (as represented by the thickness of the model cell), and

N is the total number of layers across which the well is screened.

The product Kb is the transmissivity. This transmissivity-weighted average ensures most of the water is from permeable units and the sum of the pumping from the N layers is the total pumping required. Because the conductivities of the layers were varied during parameter estimation, the volume pumped from each layer also was varied.

Assignment of model layers for high capacity wells and deep wells installed in the early 1970s was accomplished using well logs, the digital geologic model, and best professional judgment. An automated method was used to assign the model layers for all other wells. This method applied the following rules to the hydrogeologic framework model:

1. The uppermost aquifer penetrated by the well is the uppermost commingled model layer.

2. If the elevation of the well bottom is known, this elevation is used to estimate the deepest aquifer tapped. In the simple case, this aquifer is the lowermost aquifer that the well penetrated. However, if the well terminates in an overlying confining unit but penetrates 75–100 percent of its thickness, it is assumed that the underlying aquifer is hydraulically connected to the well, because wells generally terminate when a productive aquifer is located.

3. If the elevation of the well bottom is not known, but there are other wells in the quarter-quarter section for which the well bottom elevations are known, the median value is used to estimate the deepest aquifer tapped. If there are no known values, it is assumed that only the uppermost aquifer is tapped. This assumes that for domestic use, drilling will be terminated at the shallowest aquifer.

E.3—Hydraulic Conductivity and Storage Coefficients

There are 16 hydraulic conductivity zones defined in the model. Fifteen of these zones represent hydrogeologic units, with the remaining zone representing pseudo-cells. These pseudo-cells are used to facilitate flow connection between model layers where an intervening layer has pinched out, and therefore is not present. They are 1-ft thick cells with high vertical conductivity and low horizontal conductivity, simulating direct vertical hydraulic connection between the model layers. Use of these pseudo-cells allows the representation of each model layer as a distinct hydrogeologic unit.

Model layers 3–14 are each represented by one hydraulic conductivity zone each, totaling 12 zones. Where glaciofluvial deposits exist, both model layers one and two belong to a single zone. Otherwise, layer one is used to represent the poorly-sorted, relatively low-permeability upper part of the Chenoweth formation, and layer two is used to represent the higher permeability aquifer reported to occur in some parts of the Chenoweth Formation. In every instance, highly permeable model layers are adjacent to low permeability layers. This geometry ensures that vertical groundwater flow will be controlled by low permeability units and horizontal groundwater flow will be controlled by highly permeable units. For the modified transient analysis of commingling wells, all 16 zones were modeled with isotropic hydraulic conductivity, and for the model used to examine management scenarios, the Upper Undifferentiated Overburden (fig. 3) was modeled as anisotropic. The change for the Upper Undifferentiated Overburden was made to address limitations of the model for assessing the value of management scenarios (see Separation of Pumping and Commingling Effects).

The vertical hydraulic conductivity of commingling wells was defined using 16 additional zones, one corresponding to each of the 16 hydrogeologic unit zones previously defined. For each of these additional zones, horizontal hydraulic conductivity was tied to the horizontal hydraulic conductivity of the corresponding hydrogeologic unit zone, and vertical hydraulic conductivity was allowed to represent the effective hydraulic conductivity of the commingling wells. The vertical hydraulic conductivity was assumed to be the same constant value for every well cell, resulting in a single parameter to be investigated, even though vertical well hydraulic conductivity is a function of well diameter and hydraulic gradient between aquifers. It is a reasonable assumption that only one well exists in each 500-ft grid cell, and although it would be practical to compute the effect of well radius, it was not practical to adjust hydraulic conductivity as a function of hydraulic gradient. The effect of well diameter and hydraulic head difference are discussed below when establishing acceptable parameter ranges for the calibration process (see Expected and Calibrated Commingling Well Conductivity, appendix E.5).

Storage coefficients were assigned in the same manner as hydraulic conductivity. Each of the 15 hydrogeologic units and the single pseudo-cell zone has a specific storage and specific yield defined, totaling 32 zones that are coincident with the hydraulic conductivity zones.

E.4—Model Implementation

The parameterization of the model provides a flexible formulation of the conceptual problem that can be used to test the influence of any of the flow features. The model was calibrated, then it was used as a predictive tool in various ways. To systematically explore the model using computer assisted methods (Hill and Tiedeman, 2007), the model independent parameter estimation and prediction software, PEST (Doherty, 2005, 2010), was used. As implemented, PEST required three main groups of information: parameters, observations, and prior information. The parameters are described in the section Groundwater-Flow Model Analyses, with additional detail provided in appendix sections E.2 and E.3. Observations used include groundwater levels and estimates of groundwater contributions to streamflow (summarized in the Calibration section). Parameters and prior information together define the model parameterization. Prior information describes *a-priori* estimates of parameters and relations between parameters that can be described in equations.

Selection of Parameters to Estimate

The parameters to be tested are summarized in table E1 and the Tikhonov regularization (Doherty, 2005) conditions between parameters are summarized in table E2. As defined, the maximum number of adjustable parameters to be investigated was initially 115 for transient scenarios and 100 for steady-state scenarios. The number of adjustable parameters was further reduced following preliminary model calibration.

Table E1. Summary of parameter groups used in the groundwater model.

Parameter group	Physical relevance
Hydraulic conductivity of each of the 15 hydrogeologic units.	The rate at which water may be transmitted through the associated unit.
Vertical hydraulic conductivity of commingling well cells.	This represents the rate at which water may be transmitted through the well borehole from one aquifer to another.
Horizontal flow barrier conductance (hydraulic characteristic value) for each of the 48 fault segments.	This represents how easily water may pass through a fault. If conductance is high relative to hydrogeologic unit that it cuts, then the fault does not impede flow; but if conductance is low enough to impede flow, the fault is important in controlling flow.
Drain conductance for each of the 15 hydrogeologic units	Each unit has a separate drain parameter, because the ease with which water drains is assumed to be related to the unit's hydraulic properties.
Stream conductance *fraction* for each of the 15 hydrogeologic units.	It is assumed that the principle control on how easily water is gained or lost to streams is controlled by which hydrogeologic unit it is in hydraulic connection with. An initial best guess of stream conductance was made using stream geometry and an estimate of stream bed conductivity. The stream conductance fraction is a multiplier for each hydrogeologic unit that modifies the cell-by-cell initial best guess of stream conductance.
Recharge *fraction* dependent upon which layer is encountered as the uppermost model layer. There are six parameters, one for each major aquifer that occurs at the land surface.	This allows testing the assumption that recharge to any given unit occurs as predicted by the PRMS model. There are six groups, one for each major aquifer except the base of the Pomona Basalt (never occurs at land surface). The six groups are: (1) Overburden, (2) Pomona flow top and interior, (3) Selah Interbed and the upper Priest Rapids flow top and interior, (4) lower Priest Rapids flow top and interior, (5) lower interbed and Frenchman Springs flow top and interior, and (6) Grande Ronde flow top. The recharge fraction is the multiplier for the array defined by PRMS.
Specific storage terms for each of the 15 hydrogeologic units.	These represent how much water each unit stores and how water is released under the assumption each aquifer is confined. Confined versus unconfined assumptions are discussed in detail in the text.

Table E2. Physical interpretation of prior information specified in the groundwater-flow model.

[**Abbreviations**: PEST, parameter estimation software; MODFLOW, Modular finite-difference flow model; ft/d, foot per day]

Prior information statement	Physical interpretation	Relative weight
The drain conductance of the Pomona flow bottom and both Priest Rapids flow top aquifers is the same.	Because these are all highly permeable basalt interflow zones, it is expected that water will drain similarly from each of these.	Low
The hydraulic conductivity of each layer is the same as the next upper or lower layer of similar morphology.	If no other information is available, the best guess for the permeability of any layer is the permeability of the layer that was deposited under the most similar conditions. Further, if there is a trend in conductivity, it will likely occur with depth due to compaction and chemical evolution of the lava flows.	High if conditions were very similar, but low if the uncertainty is high.
The hydraulic conductivity of the Pomona flow top is ten times higher than for the glacio-fluvial deposits.	It is assumed that the glacio-fluvial deposits would likely impede water flowing freely from the Pomona flow top.	Low.
The horizontal flow barrier conductance of any section is the same as the conductance of the next section above or below it.	The best estimate of how easily a fault transmits water through one layer is the ease with which it transmits water in the vertically adjacent section. Further if there is a trend in conductance, it will likely occur with depth as a result of confining pressure and chemical evolution of the lava flows.	High.
The hydraulic conductivity of the lower Dalles unit is 1,000 times greater than the upper Dalles unit horizontal conductivity.	The bottom of the Dalles unit has been documented as permeable and productive in portions of the study area, but the upper portion is much finer textured. The value was selected to give an effective horizontal to vertical conductivity ratio of 100:1, which is typical for many heterogeneous systems.	Very low.
The hydraulic conductivity of the lower Priest Rapids flow top is ~1,250 ft/d.	This estimate was computed using pump test results from Lite and Grondin (1988), and the thickness of the most likely unit from the geomodel.	Low. Since the value is a very localized sample of a very permeable portion of one of the interflows, it is uncertain if this value is representative of conductivity controlling the watershed scale flow.
The hydraulic conductivity of the Pomona flow bottom is ~2,500 ft/d.	This estimate was computed using pump test results from Lite and Grondin (1988), and the thickness of the most likely unit from the geomodel.	Extremely low. In addition to the caveats immediately above, the pump test location is very near a pinch-out of the unit, making the estimate even more uncertain.
The stream conductance fractions are 0.1.	This is a mathematical trick to aid in mathematical stability both for PEST and the MODFLOW model. Since all stream cells also contain drain cells, loss from the system may equally be achieved by increasing either drain or stream conductance. For PEST, this clarifies which parameter to adjust. For MODFLOW, high conductance of streams sometimes gives stability problems, so whenever possible, stream conductance will be minimized in favor of increases in drain conductance.	Low.

Table E2. Physical interpretation of prior information specified in the groundwater-flow model.—Continued

[**Abbreviations**: PEST, parameter estimation software; MODFLOW, Modular finite-difference flow model; ft/d, foot per day]

Prior information statement	Physical interpretation	Relative weight
Drain conductances for aquifers and the upper Dalles layer are ten times greater than hydraulic conductivities for the same hydrogeologic units.	This is purely for mathematical stability of the estimation process. This prior information prevents drain conductances from becoming arbitrarily high if these parameters become insensitive.	Low.
The horizontal hydraulic conductivity for the upper Dalles zone is 100 times greater than the vertical conductivity.	This condition was only used for generation of vulnerability maps (see Evaluation of Potential Management Options) to prevent anomalously high head values in model panel 1 from skewing results. It is consistent with typical values of anisotropy.	Low.

During model runs where recharge was also adjustable, the general behavior of the model was to shunt water to the observation-data-poor Grande Ronde aquifer when recharge was increased or to reduce the flow to the Grande Ronde when recharge was decreased. The net effect was to take excess water and shed it to the Columbia River through the lowermost aquifer. For this reason, variation of the recharge provided little insight into the governing groundwater-flow processes in the area of interest. Because recharge was estimated using an independent method, and because PRMS recharge values provide a reasonable and conservative estimate, recharge was not adjusted for most of the groundwater flow simulation model analysis. This assumption was relaxed and examined following the bulk of the analysis below.

The transient analysis was limited, so the parameterization of storage terms was never refined. Initially, it was assumed that all sedimentary units had the same specific storage coefficients and all basalt units had the same specific storage coefficients, reducing the number of free parameters from fifteen to two. Simulation runtimes for the preliminary transient model using annual stress periods were on the order of hours, with non-convergence and significant mass conservation errors for some combinations of parameters. Three different layer assumptions were evaluated: (1) Layer 1 unconfined, and all other layers confined; (2) Layer 1 unconfined, and all other layers convertible; and (3) all layers confined. Even though some simulations with an unconfined layer 1 converged faster, the general convergence properties of the model were improved by modeling all layers as confined.

Steady-state simulations were far less time-consuming and all storage terms dropped out of the mathematical formulation, greatly increasing the efficiency of the parameter estimation process. Steady-state simulations converged in approximately 10 seconds per run. To capitalize on the favorable runtimes and robust nature of the steady-state simulations, the problem was reformulated into a modified transient analysis, assuming the system is in a dynamic steady state at three distinct periods. Because this formulation is insensitive to the formulation of storage terms, and because most aquifers are confined, all model layers were simulated as confined to improve convergence during automated parameter estimation.

The final number of independently adjustable parameters for the modified transient analysis was reduced to 85 by fixing the 6 recharge parameters and tying 9 insensitive parameters to sensitive parameters in adjacent hydrogeologic units (7 insensitive drain parameters for confining units were tied to the adjacent aquifer drain parameters, the insensitive Glaciofluvial Aquifer stream parameter was tied to the Undifferentiated Overburden stream parameters, and the poorly constrained hydraulic conductivity of the Grande Ronde flow-top aquifer hydrogeologic unit was tied to the Frenchman Springs aquifer hydrogeologic unit). Numerical stability and improved convergence were accomplished by adding regularization constraints (table E2) using prior information. Weights were only high for two sets of prior information, with low weights generally reserved for prior information that was added to guide the estimation process only when mathematical expediency contradicted physical reasonableness. The high weight sets belong to prior information equations associated with hydraulic conductivity of model layers or conductance of horizontal flow barriers. In both cases, the equations merely state that the flow properties of similar units should be similar, preventing the model from achieving a good fit by giving different values to features that should behave similarly.

Details of the Predictive Uncertainty Assessment of Pumping Compared With Effects of Commingling

Establishing Confidence Intervals for Predictions

Uncertainty in model predictions was evaluated by finding sets of reasonable parameters for which the influence of commingling wells was minimized and maximized. The best fit calibrated model demonstrated that the dominant cause of declines (approximately 85 percent) could be the result of commingling (fig. 26), so it remained to find a set of reasonable parameters that fit the data almost as well, but for which commingling was minimized. A precise definition of "almost as well" was provided by using the Scheffe statistic for simultaneous estimation of parameters with non-linear confidence intervals (Hill and Tiedeman, 2007, p. 177–181). In particular, acceptable error [in terms of the weighted least-squares objective function (ϕ)] was defined using $\hat{\delta}$, corresponding to a confidence interval of greater than 95 percent that satisfies:

$$\phi \le \phi_{min} + \hat{\delta}, \quad \text{(E.6)}$$

where

ϕ_{min} is estimated as the value of ϕ from the best-fit calibrated model.

When computing simultaneous non-linear predictions, $\hat{\delta}$ may be estimated as (Doherty, 2005; Hill and Tiedeman, 2007, p. 178):

$$\hat{\delta} = NP \bullet s^2 \bullet F_\alpha \left(NP, NDF \right), \quad \text{(E.7)}$$

where

NP is the number of parameters,

s^2 is the calculated error variance,

NDF is the number of degrees of freedom, and

F_α is the F-distribution with confidence $(1-\alpha)$.

In our case, *NFD* equals the number of observations, plus the number of prior information equations, minus the number of parameters. Doherty (2005) provides the following estimate for the error variance:

$$s^2 = \frac{\phi_{min}}{NDF}. \quad \text{(E.8)}$$

Substituting (eq. E.8) into (eq. E.7), equation E.6 can be rewritten in terms of the allowable misfit between simulated and observed values by using estimates of the minimum weighted least-squares objective function, number of parameters, the degrees of freedom, and the desired confidence level:

$$\phi \le \phi_{min} \left(1 + \frac{NP}{NDF} F_\alpha \left(NP, NDF \right) \right) = \phi_{min} \left(1 + \theta \right), \quad \text{(E.9)}$$

where

θ is defined by equation E.9.

A value for θ of 2.25 corresponds to greater than 95-percent confidence for 63 observations with non-zero weight, 81 prior information statements with non-zero weight, and 85 adjustable parameters.

Predictive Objective Function

A predictive objective function was defined so that PEST could be used to find the minimal commingling well effect resulting from any set of flow model parameters that satisfy the 95-percent confidence criteria defined in the previous section (Establishing Confidence Intervals for Predictions). The effect of commingling wells is minimal if groundwater levels return to pre-development conditions following the cessation of pumping. The recovery of each well was formulated as:

$$head_j^{final} - head_j^{late} = recovery_j, \quad \text{(E.10)}$$

where

$head_j^{final}$ is the value of hydraulic head in well j after pumping is stopped,

$head_j^{late}$ is the value of hydraulic head in well j at late time under pumping conditions.

To measure simulated recovery, total recovery was formulated as:

$$\text{Total Recovery} = \sqrt{\sum_{j=1}^{M} \left(head_j^{final} - head_j^{late} \right)^2}. \quad \text{(E.11)}$$

This equation could be used as the predictive objective function except for one potentially significant drawback. When trying to maximize this function to find the set of parameters for which commingling has the minimum effect, the Total Recovery could be dominated by a large recovery in only a few wells. However, figure 9 indicates that Group 1 wells should behave similarly. This potential drawback was addressed by adding the expected recovery based on historical data and a penalty function for when wells behave dissimilarly, yielding the final form of the prediction value to minimize:

$$\psi = \sqrt{\sum_{j=1}^{M}\left(recovery_{estimated}^{final} - \left(head_j^{final} - head_j^{late}\right)\right)^2} + \tilde{\lambda}\sqrt{\sum_{j=1}^{M}\left(head_j^{final} - head_{median}^{final}\right)^2}. \quad \text{(E.12)}$$

The argument under the second radical is the penalty function computed as sum of the distances between each final hydraulic head estimate and the median value of all of the final hydraulic heads, ensuring the wells recover together. The $\tilde{\lambda}$ is a weight factor that is manually selected to ensure that the penalty function is non-negligible. This weight was varied to ensure no persistent bias occurred during predictive runs. The $recovery_{estimated}^{final}$ term was added under the first radical so that ψ is a sum of two terms that should both be minimized. All groundwater levels should return to a value between 150 and 175 ft higher, so $recovery_{estimated}^{final}$ was set to 175. The formulation is only sensitive to this value if modeled recoveries approach the selected value, and this did not occur (fig. 26).

Computation of Change in Columbia River Basalt Group Aquifer Storage for Aquifer Vulnerability Mapping and Evaluation of Management Scenarios

For the purposes of computing change in aquifer-system storage to generate vulnerability maps and to assess management options, only change in storage of CRBG basalt aquifers was computed. For each cell, the change in storage was computed as the change in hydraulic head times the area of the cell times a storage coefficient. Total change in storage was computed by summing all model cells representing hydrogeologic units of interest. A single constant value of storage coefficient consistent with specific storage of confined basalt aquifers was used for all CRBG aquifers. This is a limitation of the results, because some aquifers are unconfined and storage change occurs by filling or draining pore spaces rather than by compressing the water and the aquifer material. Future use of a groundwater-flow model with convertible layers may be preferable for some applications. The advantage of the simpler, single storage coefficient approach is that the comparative analysis of high, medium, and low vulnerability areas are independent of the values of storage terms.

E.5—Additional Observations and Limitations from Groundwater-Flow Simulation Results

This section contains an analysis of current limitations of the groundwater-flow model for replicating aquifer-system response to commingling wells over time. These observations may provide guidance for future modeling strategies in Mosier and the larger Columbia River Basalt aquifer system.

Expected and Calibrated Commingling Well Conductivity

Considering the fact that only a couple of commingling wells were installed each year between 1972 and 1976 (fig. 16), it is evident that only a few commingling wells in a vulnerable area may cause significant declines. During the calibration and predictive analyses, a range of parameters were explored, and the following general conclusions may be drawn about the effective vertical hydraulic conductivity of well cells in the model and the hydrogeologic system in general. The estimated vertical hydraulic conductivity of cells with commingling wells ranged from large insensitive values (greater than 10,000 ft/d) to sensitive values that allow the transmission of water at rates similar to basalt aquifer conductivity (about 0.2 ft/d). The vertical hydraulic conductivity of the well cells becomes sensitive in the parameter estimation when it starts to impede vertical flow, and as expected, estimated vertical hydraulic conductivity of well cells was lowest for the maximum predicted recovery scenario (fig. 26).

A-priori estimates of effective vertical hydraulic conductivity of well cells were made to ensure that the calibrated values are reasonable. This was accomplished by computing the vertical hydraulic conductivity of a 500 ft model cell that would provide equivalent Darcian flow as turbulent flow through a vertical borehole as approximated by a rough-walled pipe. Setting the flows equal to each other:

$$Q_{pipe} = Q_{Darcy} = -K_{eff}^{v} A \frac{\Delta h}{L}, \quad \text{(E.13)}$$

where

A is the area of the model cell orthogonal to flow,
Δh is the hydraulic head across the cell in the vertical direction,
L is the length over which the hydraulic head is dropped (the thickness of the cell), and
K_{eff}^{v} is the effective vertical hydraulic conductivity for which the estimate was made.

Rearranging yields:

$$K_{eff}^{v} = \frac{-Q_{pipe}L}{A\Delta h}. \quad \text{(E.14)}$$

It remains to estimate flow through a pipe subject to the same hydraulic head gradient. The Navier-Stokes equation can be solved for laminar flow in a smooth pipe (Welty and others, 1969, p. 106–109), yielding estimates of K_{eff}^{v} ranging from about 5,000 to about 25,000 ft/d for wells ranging in diameter from 8 to 12 in. diameter, respectively. However, when considering the magnitude of pre-development gradients across basalt flow interiors, turbulent flow is likely to occur in boreholes, particularly in early time after wells were installed. Historically, 70–100 ft of hydraulic head difference occurred between aquifers separated by a hundred or more feet of impermeable basalt (Lite and Grondin, 1988). Considering that the laminar flow approximation provides an upper bound, the fully turbulent flow case provides a lower bound to K_{eff}^{v}. Turbulent flow in a rough pipe can be described by the following relations (Welty and others, 1969, p. 194–200):

$$\frac{1}{\sqrt{f_f}} = 4.0\log_{10}\left(\frac{D}{e}\right) + 2.28, \quad \text{(E.15)}$$

where

D is pipe diameter,

e is pipe roughness (units of length), and

f_f is the Fanning friction factor defined by the relation:

$$h_L = 2f_f\frac{L}{D}v^2, \quad \text{(E.16)}$$

where

h_L is the hydraulic head loss expressed in units of $\frac{\Delta P}{\rho}$,

where

ΔP is the pressure gradient,

ρ is the water density, and

v is the fluid velocity.

For a hydraulic head gradient in the horizontal direction in groundwater hydrology, $\Delta h = \frac{\Delta P}{\rho g}$, allows conversion of h_L to the same notation as the Darcy formulation (eq. E.13). Q_{pipe} is this velocity times the area of the pipe, providing all relations necessary to compute K_{eff}^{v} for fully turbulent flow in rough pipes:

$$K_{eff}^{v} = \frac{\pi\sqrt{g}\left(\frac{D}{2}\right)^{\frac{5}{2}}}{A\sqrt{\frac{\Delta h}{L}}}\left[4.0\log_{10}\left(\frac{D}{e}\right) + 2.28\right]. \quad \text{(E.17)}$$

All parameters in this equation are well known, except pipe roughness, so that K_{eff}^{v} can be plotted as a function of hydraulic head gradient. The pipe roughness term has units of length and can be conceptualized as a characteristic height of projections from the pipe wall (Welty, Wicks, and Wilson, 1969). Riveted steel or concrete pipes are rougher than most pipes, with a roughness typically ranging from 0.0002 to 0.002 ft, so a somewhat conservative estimate of 0.02 ft was used to produce figure E1. This figure illustrates that the range of calibrated effective vertical conductivities is reasonable, but it also illustrates limitations of the model.

First, the parameterization assumes that all vertical well cell hydraulic conductivities are the same, but figure E1 shows that to the contrary, this is a function of gradient, and by induction, position in the watershed. For this reason, model fit can be worse for late-time simulations with a significant number of spatially diverse commingling wells that use a single value of vertical hydraulic conductivity.

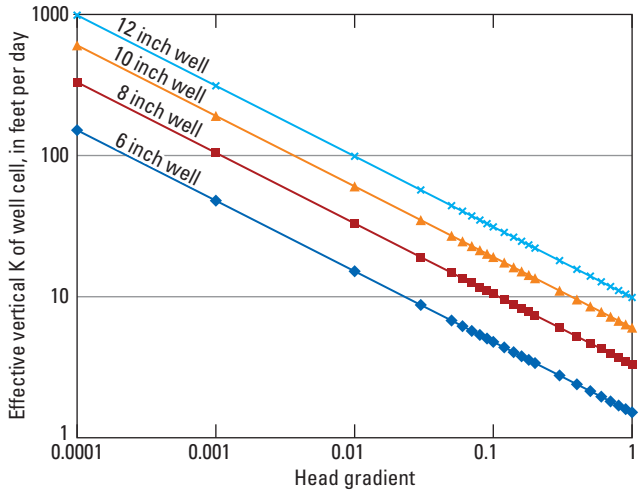

Figure E1. *A-priori* estimates of effective vertical hydraulic conductivity of well cells as a function of hydraulic head gradient. Conductance varies as a result of turbulent losses along the well borehole.

Second, the *a-priori* estimated values of vertical well cell hydraulic conductivity are in the range where sensitivity to this parameter decreases rapidly (compare the two values and sensitivities in fig. 24). The value of 0.1 ft/d (fig. 24) is approximately where flow through the well starts to become limiting, which explains why the parameter is sensitive at this value. In this context, the *a-priori* estimates (fig. E1) indicate that the wellbore itself is not likely to be flow limiting, but rather, turbulent losses within the formation as flow radially converges at the borehole may be more restrictive. Assuming that flow paths within the formation also can be represented as flow through rough pipes, equation E.17 may be used to estimate the effective diameter of pores controlling flow. The analysis was crude, but indicated that characteristic pore diameters of the rate-controlling aquifer may range from 1 to 4 in., corresponding to approximately 0.1 ft/d. Considering basalt aquifer morphology, these values appear to be reasonable. The calibrated value of well cell vertical hydraulic conductivity may be accounting for hydraulic head loss near the borehole, and not in the borehole itself.

Third, the strong dependence of the effective vertical hydraulic conductivity on the hydraulic head gradient coupled with the hydraulic head loss over time indicates any model with a constant well vertical hydraulic conductivity possibly will have severe limitations for use in a fully transient analysis. Because effective well vertical hydraulic conductivity increases as the head gradient decreases (fig. 9), the resulting drawdown curve will be flatter over time than for the response resulting from having a constant well vertical hydraulic conductivity, potentially contributing to the linear system response of the Group 1 groundwater level declines (fig. 9).

Observations from Fully Implemented Transient Simulations

During preliminary analyses, transient groundwater flow and changes in groundwater levels were simulated using monthly and annual stress periods, generally resulting in convergence problems and poor mass balances. Following the modified transient analysis used for calibration and prediction, a fully transient model was used to investigate the rate of decline observed in the OWRD administrative area. This model used the simulated head from the early-time steady-state model as the initial hydraulic head distribution, and used the late-time distribution of commingling wells to simulate time-varying system response. Because declines have been linear since the 1970s, the late-time (2006) well distribution was assumed to be sufficient for testing the model.

This modeling was accomplished to evaluate the linear nature of groundwater-level declines of CRBG aquifers in the OWRD administrative area. If a single penetration is made into a confined aquifer with a fixed elevation controlling the rate of drainage, then the time-dependent groundwater level decline is predicted to be exponential. Adding penetrations sequentially would increase the rate of decline over time, which may contribute to a more linear appearance, but would more likely result in a variable rate of decline with jumps in rate when new penetrations occur. However, measured groundwater-level time series are persistently linear, and examination of new well hydrographs show that groundwater level in the well will often drop from an initially higher value to approximately the same hydraulic head as the remainder of the group. This argues against sequential well installation as being the primary cause of the linear response, and the absence of changes in the rate of decline associated with new wells implies that the final distribution of wells is sufficient for testing the transient response of the groundwater model.

Recall that all model runs simulated confined groundwater flow in each model layer. The value of the specific storage was adjustable during automated parameter estimation to account for the drainage (specific yield) of some areas of the formations. However, only two specific storage parameters were used initially: one for all basalts and one for all sedimentary units. Early attempts at monthly simulation showed flashy system response of simulated hydraulic heads due to seasonal variations in recharge and variations between years. To reduce this effect, annual average recharge was used with annual time steps for the transient model. This is reasonable because groundwater levels indicate that seasonal and intra-annual effects are small compared to the large declines being analyzed (see the “Temporal Variation in Groundwater Levels and Changes in Groundwater Storage” section of the main report).

Because it was assumed that pre-development and early-time conditions were essentially in steady state, calibration targets for these time periods were used in the same manner as described for the modified transient analysis. Following each early-time steady-state model run, final hydraulic heads were exported to a transient model for use as initial hydraulic heads for the annual time step transient simulations, which allowed examination of system response since the early-1970s to current pumping and commingling stresses. All available hydraulic head measurement values were used. If multiple measurements were taken throughout the year, the median value was used as the annual groundwater level calibration target to de-emphasize outliers resulting from pumping conditions. Under the previous assumptions, parameter estimation using PEST was undertaken. Because groundwater-level measurements were taken at regular intervals during the entire period 1972–2006, the automated calibration was anticipated to find a set of parameters resulting in linear declines of Group 1 wells, as well as matching pre-development and early-time heads.

Using *a-priori* estimates of basalt aquifer storage coefficients resulted in rapid exponential groundwater-level declines of water levels in Group 1 wells, with the system asymptotically approaching steady state in 2–5 years. This timescale of response is similar to the time it took for water

levels in several new Group 1 wells to decline from their initial value (shortly after drilling) to values similar to other Group 1 wells (fig. 9), suggesting these wells are located in confined aquifers that were connected during well construction to a portion of the groundwater system experiencing linear declines.

During calibration, storage terms increased from true confined storage values and drainage and commingling parameters slowed water flow from the aquifer system, resulting in a best fit that exhibited an exponential rate of decline with systematic under prediction of groundwater levels in earlier time and over prediction in later time. As a result, model fit was poor, and declines were nonlinear. A suite of runs using different starting values of parameters was explored to ensure the calibration problems were not the result of poor starting values, but in all cases, the model had similar behavior. In other words, the linear declines were not reproduced using the simple two-storage coefficient (overburden and basalt) representation.

The following mechanisms are not represented in the model, and some combination of these may account for the approximately linear response of the system:

Non-Darcian flow resulting from commingling wells: Turbulent hydraulic head loss will result in lower apparent hydraulic conductivity under high gradient conditions, with well vertical hydraulic conductivity apparently increasing as hydraulic heads between aquifers equilibrate. This mechanism was discussed more completely in the previous section.

Dual storage parameters representing specific yield as well as specific storage: In a single-aquifer groundwater-flow system, this does not have a large effect, but in a multi-aquifer flow system, drainage of the one aquifer (specific yield) through commingling wells into a second confined aquifer can result in complex behavior.

The Effect of Compartmentalization on Transient Behavior

To test the efficacy of the dual storage mechanism for linearizing declines in a compartmentalized system, a simple two compartment analytical model was developed (fig. E2). Initially, the system is composed of two isolated compartments at different initial steady hydraulic heads. At time zero, each compartment is perforated, resulting in two effective conductance terms that describe how water flows between the compartments and out of the system as a function of the difference in hydraulic head across the perforated barrier. Perforation of the compartments connects compartment 1 with compartment 2 and compartment 2 with a fixed hydraulic head condition outside the system. It is assumed hydraulic head in compartment 1 is greater than hydraulic head in compartment 2, which is in turn, greater than hydraulic head outside the system.

This geometry is a simplified representation of the case where deep basalt aquifers are at a higher hydraulic head than shallow basalt aquifers, and where commingling wells create a conduit to a constant elevation outflow such as what is presumed to exist near Group 1 wells. It is a reasonable representation for the case where flow between the aquifers is more restrictive than flow through the aquifers themselves. The method of solving the following differential equations guarantees that the general solution may be written as the sum of the solutions to the homogeneous equations and the particular solutions (Powers, 1987). The solution to the homogeneous equations defines the transient response of the system with final steady-state heads defined by the particular solution, which is determined by the recharge rate and the conductance out of each compartment. Because we are interested in examining the time-varying response of the system, it is sufficient and simplest to examine the solution to the homogeneous equations. The solution to the homogeneous equation for each compartment is a good approximation to the general solution for the case where the leakage rate is much greater than the recharge rate.

The equation describing hydraulic head in compartment 1 is:

$$\hat{S}_1 \frac{dh_1}{dt} = -C_{1\leftrightarrow 2}\left(h_1 - h_2\right), \qquad \text{(E.18)}$$

where

$\hat{S}_1$ is a coefficient describing storage of compartment 1,

h_1 and h_2 represent the hydraulic heads in compartments 1 and 2, respectively, and

$C_{1\leftrightarrow 2}$ is the conductance between compartments 1 and 2.

Similarly, hydraulic head in compartment 2 is described by:

$$\hat{S}_2 \frac{dh_2}{dt} = C_{1\leftrightarrow 2}\left(h_1 - h_2\right) - C_{2\leftrightarrow f}\left(h_2 - h_f\right). \qquad \text{(E.19)}$$

The final hydraulic head to which the system will equilibrate (h_f) is controlled by the elevation of the outfall and can be set to any arbitrary datum defining the elevation from which all other hydraulic heads are measured. For this analysis, it is set to zero, simplifying equation (E.19) to:

$$\hat{S}_2 \frac{dh_2}{dt} = C_{1\leftrightarrow 2}\left(h_1 - h_2\right) - C_{2\leftrightarrow f} h_2. \qquad \text{(E.20)}$$

The conductance across each barrier is the change in volumetric flux per unit change in hydraulic head across the barrier, giving units of length squared per time. The coefficient describing storage of each compartment is equal to the volume of water released per unit change in hydraulic head, or in hydrogeologic terms:

Two-compartment Model

Initial Condition = Two sealed compartments

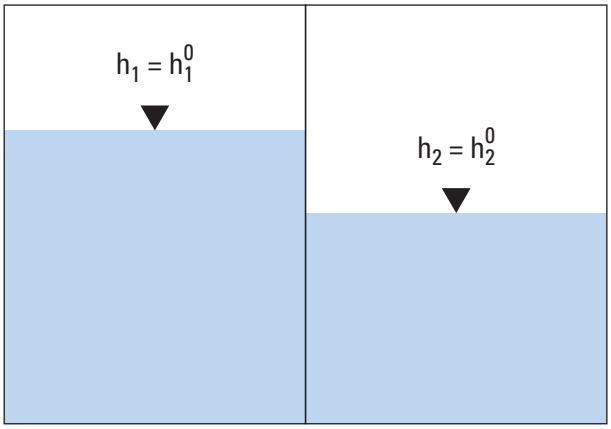

Transient Condition = Both compartments have been perforated

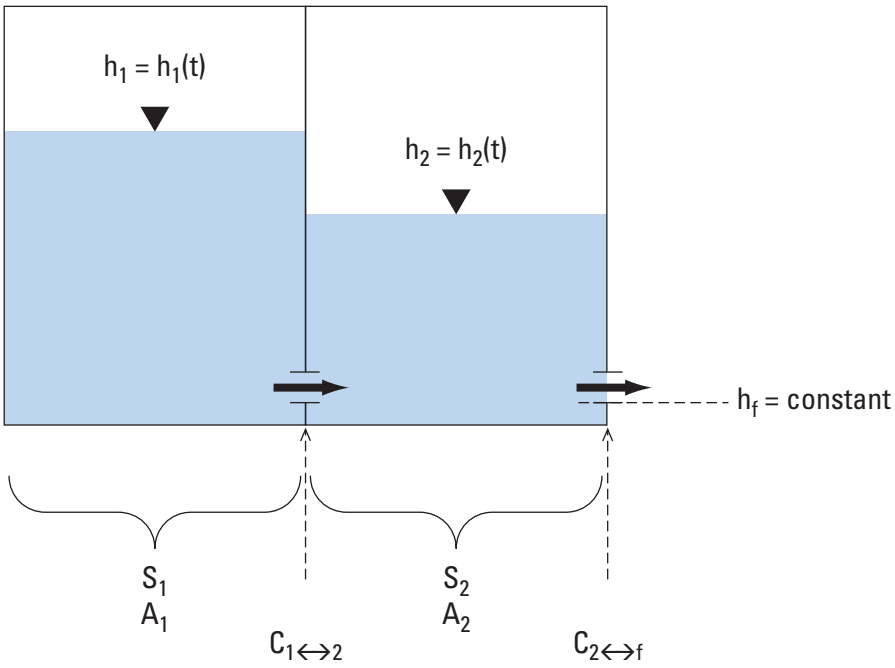

Properties:
- **Storativity**
- **Area**
- **Conductance**

Figure E2. A two-compartment model.

$$\hat{S}_k = A_k S_k, \tag{E.21}$$

where

A_k is the plan view area of compartment k, and

S_k is the storativity (the usual storage coefficient used in groundwater flow equations) of compartmen k.

Writing the equations (eq. E.18) and (eq. E.20) in terms of one independent variable each yields:

$$S_1 A_1 S_2 A_2 \frac{d^2 h_1}{dt^2} + \left[\left(C_{1\leftrightarrow 2} + C_{2\leftrightarrow f} \right) S_1 A_1 + C_{1\leftrightarrow 2} S_2 A_2 \right] \frac{dh_1}{dt} + C_{1\leftrightarrow 2} C_{2\leftrightarrow f} h_1 = 0, \tag{E.22}$$

and

$$S_1 A_1 S_2 A_2 \frac{d^2 h_2}{dt^2} + \left[\left(C_{1\leftrightarrow 2} + C_{2\leftrightarrow f} \right) S_1 A_1 + C_{1\leftrightarrow 2} S_2 A_2 \right] \frac{dh_2}{dt} + C_{1\leftrightarrow 2} C_{2\leftrightarrow f} h_2 = 0. \tag{E.23}$$

If the storativities and conductances are known, both equations are homogeneous second order ordinary differential equations with unique solutions of the form:

$$h_1 = B_1 e^{m_1 t} + B_2 e^{m_2 t}, \tag{E.24}$$

and

$$h_2 = B_3 e^{m_1 t} + B_4 e^{m_2 t}. \tag{E.25}$$

With m_1 and m_2 being the two roots of x for the following equation:

$$S_1 A_1 S_2 A_2 x^2 + \left[\left(C_{1\leftrightarrow 2} + C_{2\leftrightarrow f} \right) S_1 A_1 + C_{1\leftrightarrow 2} S_2 A_2 \right] x + C_{1\leftrightarrow 2} C_{2\leftrightarrow f} = 0. \tag{E.26}$$

Additionally, the B coefficients are provided by solving the initial value problem with two initial conditions for each equation. The initial conditions are that hydraulic head in each compartment is known, and the instantaneous flux honors the following conductance based formulation, which is assumed to hold for all time following perforation:

$$h_1 \left(t = 0 \right) = h_1^0, \tag{E.27}$$

$$S_1 A_1 \frac{dh_1 \left(t = 0 \right)}{dt} = -C_{1\leftrightarrow 2} \left(h_1^0 - h_2^0 \right), \tag{E.28}$$

$$h_2 \left(t = 0 \right) = h_2^0, \tag{E.29}$$

$$S_2 A_2 \frac{dh_2 \left(t = 0 \right)}{dt} = C_{1\leftrightarrow 2} \left(h_1^0 - h_2^0 \right) - C_{2\leftrightarrow f} h_2^0. \tag{E.30}$$

This initial boundary value problem was solved for a set of parameters representing the storage properties (area and storativity values representative of specific storage and specific yield) of the Mosier system, allowing assessment of fitted parameters for reasonableness (table E3). All units are in feet and days to allow easy comparison with MODFLOW parameters. The area of compartment 1 is assumed to be a square approximately 6 miles on a side, and compartment 2 is one-half the area corresponding to the approximate size of the lower and upper aquifers respectively. Initial head for compartment 2 was fixed at 300 ft, which corresponds to the approximate head difference between the uppermost aquifers and the elevation of Mosier Creek in the OWRD administrative area prior to 1970. Initial head for compartment 1 and both conductance terms were fitting parameters. Two scenarios were considered for storage terms (table E3): (1) both compartments are assumed to have an equal confined or pseudo-confined value (*equal storage* [table E3; fig. E3]); and (2) compartment 1 is assumed to release water through drainage (specific yield), and compartment 2 has the confined or pseudo-confined value (*unequal storage* [table E3; fig. E3]). Pseudo-confined is defined as a larger than anticipated value for true confined conditions. The specific yield of compartment 1 is fixed at 0.2, and the role of the magnitude of the confined or pseudo-confined storage terms is varied to examine the role of this term on system response (fig. E3).

The starting head in compartment 1 and the conductance terms were varied to achieve an approximately linear decline of 175 ft during a 30 year period, yielding reasonable physical values for both initial head and conductance. Because it is not certain whether water leaks more easily from the commingled basalt system or more easily between the basalt aquifers within the system, both cases were examined by varying conductance in a fixed ratio during exploration of parameter values.

If more commingling wells are present in the geologically higher aquifers, then conductance could be higher between compartment 2 and the outfall than between the compartments. This corresponds to figures E3*D* through *F*, where conductance to the outfall is assumed to be twice the conductance between the compartments. The other case is where conductance between the compartments is higher than conductance to the outfall. Because all wells have a sanitary seal, flow up and out the boreholes has to pass through the uppermost geologic units. In most cases, it is feasible that these units provide more resistance to flow than is experienced by the borehole itself, so to test the feasibility of this case, conductance of the outfall was assumed to be 60 percent of conductance between the compartments (figs. E3*A*–*C*).

Table E3. Values tested to demonstrate that compartmentalization using reasonable parameter values can help explain the long term linear declines of Group 1 wells.

[**Abbreviations:** ft, foot; ft^2/d, foot squared per day; ft^2, square foot]

Parameter		Figure E3A	Figure E3B	Figure E3C	Figure E3D	Figure E3E	Figure E3F
Initial head in compartment 1 (h_1^0; units = ft)		500	500	500	900	900	900
Initial head in compartment 2 (h_2^0; units = ft)		300	300	300	300	300	300
Conductance between compartments 1 and 2 ($C_{1\leftrightarrow 2}$; units = ft^2/d)		4.90×10^4	4.90×10^4	4.90×10^4	2.45×10^4	2.45×10^4	2.45×10^4
Conductance between compartment 2 and the system outfall ($C_{2\leftrightarrow f}$; units = ft^2/d)		2.94×10^4	2.94×10^4	2.94×10^4	4.90×10^4	4.90×10^4	4.90×10^4
Storage coefficient of compartment 1 (S_1; unitless)	*Equal storage*	1.0×10^{-2}	1.0×10^{-3}	1.0×10^{-6}	1.0×10^{-2}	1.0×10^{-3}	1.0×10^{-6}
	Unequal storage	0.20	0.20	0.20	0.20	0.20	0.20
Storage coefficient of compartment 2 (S_2; unitless)		1.0×10^{-2}	1.0×10^{-3}	1.0×10^{-6}	1.0×10^{-2}	1.0×10^{-3}	1.0×10^{-6}
Area of compartment 1 (A_1; units = ft^2)		1.0×10^9	1.0×10^9	1.0×10^9	1.0×10^9	1.0×10^9	1.0×10^9
Area of compartment 2 (A_2; units = ft^2)		5.0×10^8	5.0×10^8	5.0×10^8	5.0×10^8	5.0×10^8	5.0×10^8

The set of values tested (table E3) demonstrates that compartmentalization using reasonable initial conditions and parameter values can help explain the long term linear declines of Group 1 wells for a range of storage parameter contrasts (fig. E3). For both conductance conditions (compare columns of fig. E3), an approximately linear decline of about 175 ft over 30 years occurs in compartment 2 for the unequal storage case. Further, the effect of varying the confined or pseudo-confined storage term has negligible effect on the unequal storage response as long as this parameter is at least 20 times smaller than the specific yield, indicating that the aquifer being drained controls the rate of decline. As the magnitude of the pseudo-confined storage approaches the specific yield, the solution to the equations becomes sensitive to the volume of water in compartment 2.

The range of 500 to 900 ft for initial hydraulic heads in compartment 1 is reasonable given measured hydraulic heads high in the watershed and anecdotal evidence of hydraulic gradients in the OWRD administrative area. The model predicts that these maximum hydraulic head values only need to have existed prior to aquifer cross-connection. Variations in initial hydraulic head for compartment 1 account for short term increases or declines in compartment 2 hydraulic head following cross-connection events. For example, figures E3*A* through *C*, show a minor increase in hydraulic head initially, but lowering initial hydraulic head in compartment 1 to 475 ft eradicates the early-time rise with only a small effect on the remainder of the hydrograph.

To evaluate the magnitude of the conductance terms for reasonableness, Darcy's flow law is compared to the conductance formulation. Setting these equal to each other:

$$-C_{1\leftrightarrow 2}\left(h_1 - h_2\right) = -K_v^{wells} A \frac{\left(h_1 - h_2\right)}{L}, \tag{E.31}$$

where

A is the area through which the commingling flow occurs, and

L is the thickness of the barrier penetrated by the well.

The area is the number of well cells (n) times the cell area (250,000 ft^2), yielding:

$$K_v^{wells} = \frac{C_{1\leftrightarrow 2} L}{250{,}000 n}. \tag{E.32}$$

Taking the highest value of conductance from table E3, and assuming a reasonable value of L for a typical vertical distance between aquifers (approximately 100 ft), yields:

$$K_v^{wells} \approx \frac{20}{n} \text{ feet per day.} \tag{E.33}$$

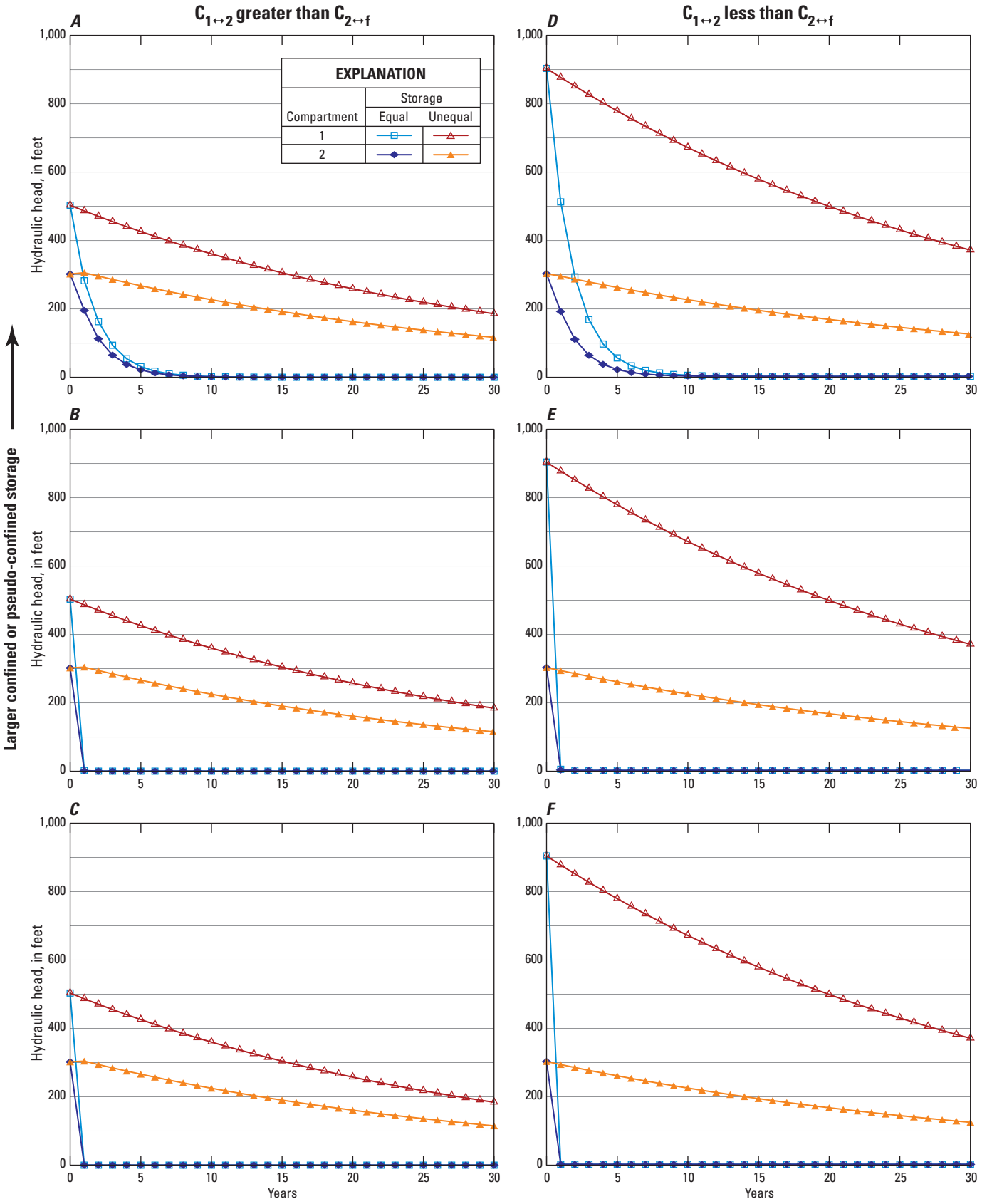

Figure E3. Hydraulic head response in a two-compartment model under various conditions summarized in table E3.

This implies that one well at 20 ft/d, two wells at 10 ft/d, or 20 wells at 1 ft/d would all provide conductance values consistent with the analytic model. Even one well at 20 ft/d is reasonable given the *a-priori* estimates of conductivity (fig. E1) and falls within the range of calibrated values from the MODFLOW model (fig. 24) and the number of potentially commingling wells (fig. 16). Because both cases considered provided reasonable starting hydraulic head values and conductance values, the model is robust in either case, and both working hypotheses must be retained.

Two final comments on the analytic model are instructive. First, the analytic model is generally insensitive to the size of compartment 2 (data not shown). This is because the source of water controlling the rate of decline is compartment 1. Second, if storativity in compartment 2 also is set to a value of specific yield, then the results are virtually indistinguishable from only using specific yield in compartment 1 (for the conditions analyzed). This again is the result of compartment 1 supplementing compartment 2. However, this begs the question: Why did parameter estimation using the MODFLOW model not drive storage to values consistent with unconfined conditions? This is because there are many more wells besides Group 1 wells for which calibration targets were used. The response of these other wells also places constraints on the model calibration, and the net result is that a single storage parameter is not viable for the entire model area. Use of convertible layers to allow simulation of unconfined conditions allows use of multiple parameters without prior knowledge of which aquifers will drain to supplement other aquifers.

The key conclusions from the analytic model are that compartmentalization and draining of one aquifer to supplement another are viable mechanisms to explain the long-term linear declines of group 1 wells. Additionally, a groundwater-flow model capable of simulating unconfined conditions for all aquifers could be used to test the hypothesis that long-term linear declines are the result of supplementing lower hydraulic head aquifers by draining higher hydraulic head aquifers.